

Improvement in electrical properties of hafnium and zirconium silicates by postnitriding

This article has been downloaded from IOPscience. Please scroll down to see the full text article.

2006 J. Phys.: Condens. Matter 18 6009

(<http://iopscience.iop.org/0953-8984/18/26/019>)

View [the table of contents for this issue](#), or go to the [journal homepage](#) for more

Download details:

IP Address: 129.252.86.83

The article was downloaded on 28/05/2010 at 12:00

Please note that [terms and conditions apply](#).

Improvement in electrical properties of hafnium and zirconium silicates by postnitriding

T Ito¹, H Kato², T Nango¹ and Y Ohki¹

¹ Department of Electrical Engineering and Bioscience, Waseda University, Shinjuku-ku, Tokyo 169-8555, Japan

² Diamond Research Center, National Institute of Advanced Industrial Science and Technology (AIST), Umezono, Tsukuba-shi, Ibaraki 305-8565, Japan

E-mail: prince@suou.waseda.jp

Received 15 February 2006, in final form 6 May 2006

Published 19 June 2006

Online at stacks.iop.org/JPhysCM/18/6009

Abstract

Hafnium and zirconium silicate films were deposited on a silicon substrate and the effects of postannealing on their electrical properties were investigated. When the films are postannealed in nitrogen monoxide (NO), the leakage current becomes lower by more than one order of magnitude as compared with that of the as-deposited films. The capacitance–voltage (C – V) hysteresis width is also decreased drastically by the NO postannealing. From electron spin resonance spectroscopy, it is indicated that paramagnetic defects at the interface between the film and the substrate are responsible for the leakage current and the C – V hysteresis. It is also indicated by x-ray photoelectron spectroscopy that the postnitridation effectively terminates these interface defects and contributes to the improvement in electrical properties.

1. Introduction

According to guidelines for manufacturing processes for the future complementary metal–oxide–semiconductor (CMOS) technology such as the International Technology Roadmap for Semiconductors (ITRS), the thickness of the gate silicon dioxide is expected to be scaled down to a value below its thinnest limit in the near future [1]. In this thickness region, silicon dioxide would not maintain its insulating property, since direct tunnelling dominates the leakage current [2, 3]. In order to overcome this difficulty, several attempts to increase the physical thickness have been carried out using materials with a higher permittivity, while keeping the equivalent silicon dioxide thickness unchanged [4–6]. However, these materials contain various densities of defects, many of which will get charged and cause an increase in their leakage currents. Therefore, finding an adequate method to improve their electrical properties is necessary.

We have successfully deposited hafnium silicate and zirconium silicate by plasma-enhanced chemical-vapour deposition (PECVD) and examined their energy band profiles and

photoluminescence characteristics [7, 8]. In the present paper, we investigate the effects of postannealing on their electrical properties, in order to find a clue to the improvement.

2. Samples and experimental procedures

Hafnium silicate and zirconium silicate films were deposited using a PECVD technique. The source gases were tetraethoxysilane [TEOS: $\text{Si}(\text{OC}_2\text{H}_5)_4$] and a hafnium alkoxide [$\text{Hf}(\text{O}-i\text{-C}_3\text{H}_7)_4$] or a zirconium alkoxide [$\text{Zr}(\text{O}-i\text{-C}_3\text{H}_7)(\text{C}_{11}\text{H}_{19}\text{O}_2)_3$]. Oxygen, used as an oxidation gas, was excited with an rf power of 13.56 MHz through capacitive coupling. The TEOS was vaporized and transported at 70 °C into the ‘tail flame’ of the oxygen plasma. The hafnium or zirconium alkoxide was vaporized and transported at 220 °C into the oxygen plasma using argon gas as a carrier and diluent gas. The gas flow rate was controlled with a mass-flow controller. The films were deposited onto a p-type silicon monocrystal wafer (100) set on a stage whose temperature was kept at 400 °C.

The elemental composition and chemical structure of the deposited films were estimated through x-ray photoelectron spectroscopy (XPS, JEOL JPS-9010TR) and x-ray diffraction (XRD) spectroscopy (Rigaku RAD-IC). The XPS peaks ascribable to Hf–O–Si or Zr–O–Si bonds appeared, while no peaks to be ascribed to Hf–Si or Zr–Si silicide bonds were seen. No crystalline peaks appeared in the XRD spectra of both silicates. Therefore, the deposited films were confirmed to be amorphous silicates with the chemical formula $\text{Hf}_{0.43}\text{Si}_{0.57}\text{O}_{1.8}$ or $\text{Zr}_{0.32}\text{Si}_{0.68}\text{O}_{2.0}$. Here, the estimation error in the chemical composition is about 10%. The film thickness was measured to be about 80 nm for both silicates by ellipsometry (Ulvac ESM-1) with a He–Ne laser at a wavelength of 632.8 nm.

For postannealing, the deposited films were kept at 900 °C for 60 s in a rapid thermal annealing apparatus filled either with nitrogen monoxide (NO), oxygen (O_2) or nitrogen (N_2) at a pressure of $\sim 1.0 \times 10^5$ Pa. The postannealing in NO is known to cause nitridation and oxidation, while that in O_2 causes oxidation [9, 10]. No such chemical changes are expected in the N_2 postannealing.

Fourier transform infrared (FT-IR) absorption spectroscopy was carried out before and after the postannealing in a JEOL JIR-WINSPEC50 spectrometer. On the other hand, electron spin resonance (ESR) spectra were examined for the samples put in a pure silica glass cell with a JEOL JES-FA 300 spectrometer at the X-band frequency at room temperature in air. In order to obtain the g -values, a standard Mn^{2+} signal marker was used. The number of paramagnetic spins was evaluated by double numerical integration of a first-derivative ESR spectrum and by comparison with the signal from diphenylpicrylhydrazyl ($g = 2.0036$) of a known weight. The accuracy of estimation is believed to be $\pm 20\%$.

Electrical properties were examined at room temperature for the sample having a metal–insulator–semiconductor structure consisting of the lower silicon substrate, the film and an evaporated gold upper electrode with an effective area of 2.8×10^{-3} cm². The leakage current was measured using a high resistance meter (Advantest R8340) by applying a positive dc voltage to the upper electrode while changing its average field value from 0 to 14 MV cm⁻¹ in a stepwise manner with a step of 0.03 MV cm⁻¹. The capacitance–voltage (C – V) characteristics were obtained at 1 MHz using a high-frequency C – V meter (Sanwa Mega Bytec MI-494) by sweeping the voltage first from negative to positive at a constant rate of 0.4 V s⁻¹ and then by sweeping it inversely.

3. Results and discussion

Figure 1 shows the current density J as a function of the electric field intensity E obtained for the hafnium and zirconium silicates. The J – E curves clearly vary for the different

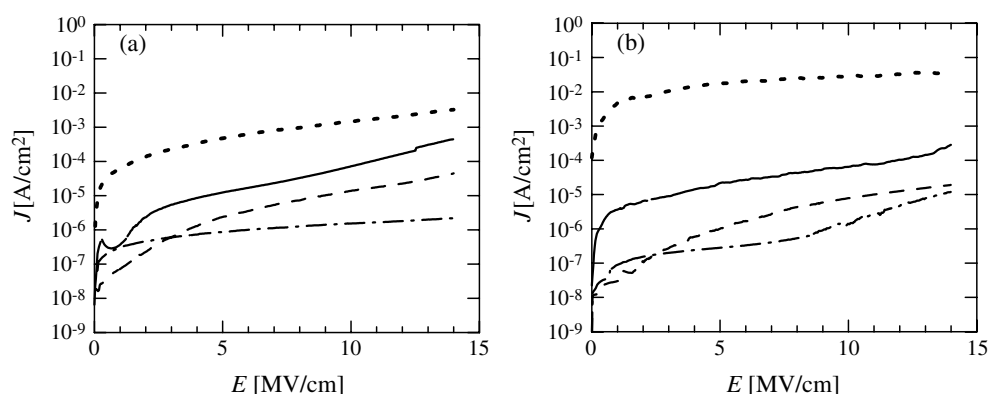


Figure 1. (a) Relations between the electric field intensity E and the current density J observed for hafnium silicate before (solid curve) and after postannealing in NO (dashed–dotted curve), O_2 (dashed curve) or N_2 (dotted curve). (b) Similar relations observed for zirconium silicate before (solid curve) and after postannealing in NO (dashed–dotted curve), O_2 (dashed curve) or N_2 (dotted curve).

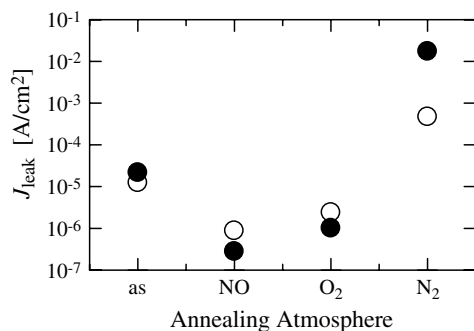


Figure 2. Changes in the leakage current density J_{leak} with the difference in the postannealing atmosphere. Open and closed symbols are the data obtained for hafnium silicate and zirconium silicate, respectively.

postannealing atmospheres. For both silicates, J becomes smallest in the case of O_2 annealing at $E < 3 \text{ MV cm}^{-1}$. However, at $E > 3 \text{ MV cm}^{-1}$, J is most effectively reduced by the NO annealing. According to ITRS, CMOS devices with a SiO_2 gate dielectric film are to be operated at 10 MV cm^{-1} [1]. The permittivity values of the present silicate samples were measured to be about 7, nearly twice as high as that of SiO_2 . Therefore, the equivalent thickness of the present film turns out to be twice the SiO_2 thickness. Therefore, it would be better to compare the leakage current density J_{leak} at $E = 5 \text{ MV cm}^{-1}$. The changes in J_{leak} due to the difference in the postannealing atmosphere are compared in figure 2 for the two silicates. Regardless of whether the sample is hafnium or zirconium silicate, the value of J_{leak} is lower in the NO and O_2 postannealed samples than in the as-deposited samples, whereas it is higher in the N_2 postannealed samples. In particular, in the NO postannealed samples, J_{leak} decreases by more than one order of magnitude as compared to the value in as-deposited samples. Therefore, it is clear from figure 2 that the NO postannealing is quite effective in reducing J_{leak} in both the silicates.

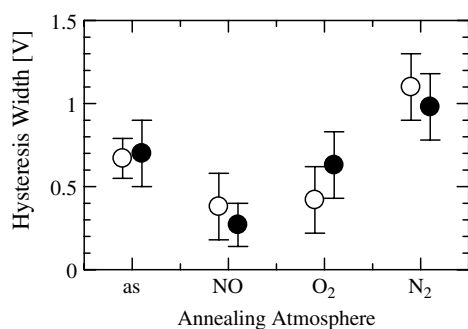


Figure 3. Changes in the hysteresis width with the postannealing atmosphere. Open and closed symbols are the data obtained for hafnium silicate and zirconium silicate, respectively.

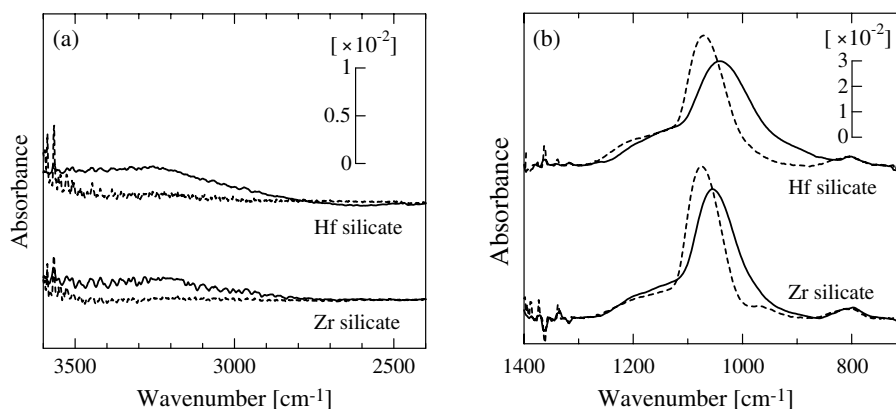


Figure 4. FT-IR spectra obtained for hafnium and zirconium silicates from 2400 to 3600 cm^{-1} (a) and around 1000 cm^{-1} (b). The solid and broken curves are the spectra before and after the postannealing in NO, respectively.

Figure 3 shows the C - V hysteresis widths measured before and after the postannealing. For both silicates, the width decreases with NO or O_2 postannealing, whereas it increases with N_2 postannealing. This changing pattern is very similar to that of J_{leak} shown in figure 2. The hysteresis width is known to reflect the number of charge traps in the bulk or at the interface [11, 12]. Therefore, the decrease in the number of charge traps, which can act as leakage paths for carriers, is considered to bring about a lower leakage current.

In order to investigate the reasons for the changes in J_{leak} and in the hysteresis width with the postannealing atmosphere, FT-IR and ESR measurements were carried out. Figure 4 shows FT-IR spectra obtained before and after the postannealing in NO. The absorption peaks around 1000 and 3400 cm^{-1} seen in the as-deposited samples are attributable to Si-O and OH bonds, respectively. Here, the OH bonds seem to be contained as impurities in the samples. In figure 4, the OH bonds clearly disappear with NO postannealing. Similar disappearance was confirmed in the O_2 and N_2 postannealed samples, although the spectra are not shown here. This means that hydrogen-related impurities are desorbed by the postannealing, regardless of its atmosphere.

The wavenumber K of the FT-IR absorption peak around 1000 cm^{-1} due to Si-O bonds can be an indicator of the structural distortion. The bond angle $\angle\text{SiOSi}$, denoted by θ , is known

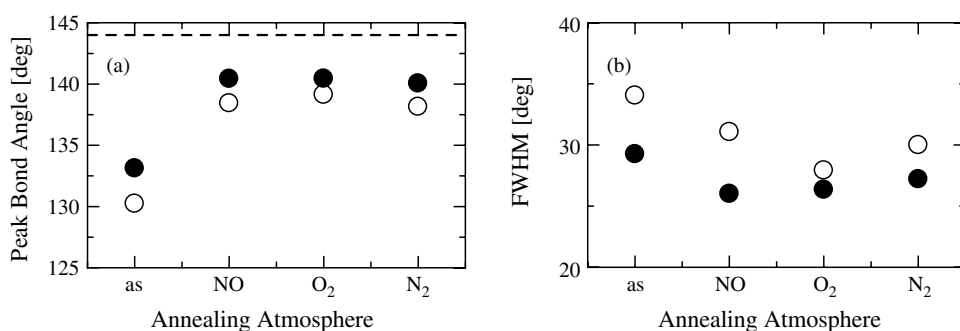


Figure 5. Changes in the peak value (a) and FWHM (b) of the bond angle $\angle\text{SiOSi } \theta$ with the postannealing atmosphere. Open and closed symbols represent the data obtained for hafnium silicate and zirconium silicate, respectively. The broken line in (a) is drawn as a guide to the eyes to show the value of 144° .

to follow the equation [13]

$$K = a \left[\frac{2}{m} \left(\alpha \sin^2 \frac{\theta}{2} + \gamma \cos^2 \frac{\theta}{2} \right) \right]^{1/2}. \quad (1)$$

Here, K is in cm^{-1} , a and γ are constants ($5.3 \times 10^{-12} \text{ s cm}^{-1}$ and 100 N m^{-1} , respectively) and m is the mass of an oxygen atom. The α -value might in principle be able to vary with the modification of the bond length of Si–O, $d_{\text{Si-O}}$. However, it has been reported that the major cause of K variation is due to θ and not to changes in α through $d_{\text{Si-O}}$ for the range $120^\circ < \theta < 150^\circ$ in the case of silicate materials [13]. Therefore, variations in $d_{\text{Si-O}}$ and α are neglected and α is regarded as a constant value of 600 N m^{-1} [13]. By substituting K into equation (1), the FT-IR spectra were converted to those expressed as a function of θ . Figure 5 shows the peak value and the full width at half maximum (FWHM) of θ of such converted spectra. The peak bond angle approaches 144° , the most stable value of θ [13], for all the postannealing atmospheres. The value of FWHM also decreases with postannealing. Therefore, it is clear that the postannealing reduces the randomness in microscopic structure regardless of its atmosphere. The desorption of hydrogen-related impurities by the postannealing seems to play a role in the structural stabilization. However, since the dependences of J_{leak} and the hysteresis width on the annealing atmosphere shown in figures 2 and 3 are not similar to those of the peak value and FWHM of θ shown in figure 5, the structural randomness seems to have no direct relation to the electrical properties.

Figure 6 shows ESR spectra obtained in zirconium silicate before and after postannealing. Although not so clear, the spectra are presumed from their shapes and g -values to be due to the P_b centre, which is an inherent point defect induced by a lattice mismatch at an interface between Si and SiO_2 [14]. Figure 7 shows the change in the number of paramagnetic spins with postannealing estimated from figure 6. The NO annealing effectively eliminates the defects, while the N_2 annealing increases their number. This dependence of the spin number on the annealing atmosphere is similar to those of J_{leak} and the hysteresis width shown in figures 2 and 3. Therefore, it is highly probable that the defects causing the ESR spectra at the interface between the silicon substrate and the film are responsible for the increase in the leakage current and the hysteresis width.

To verify this assumption further, we now discuss how the NO postannealing reduces the number of interface defects. Since these interface defects are observable by ESR as shown in

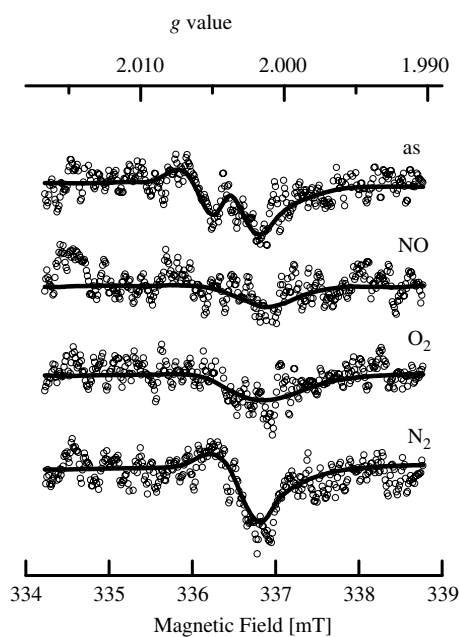


Figure 6. ESR spectra obtained for zirconium silicate before and after postannealing. The solid curves are drawn as a guide for the eyes.

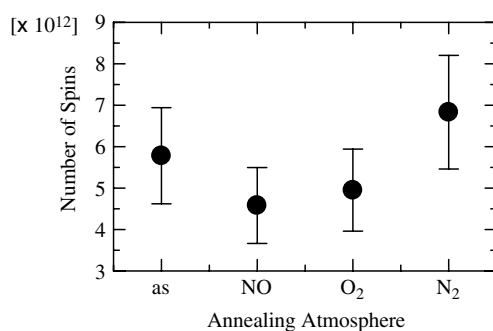


Figure 7. Change in the number of spins with the postannealing atmosphere obtained for zirconium silicate.

figure 6, they should have unpaired electrons. For SiO_2 deposited on a Si substrate, it has been reported that unpaired P_b centres at SiO_2/Si interfaces are terminated by the NO annealing, forming $\text{Si}_3\equiv\text{N}$ bonds and $\text{Si}_2=\text{N}-\text{O}$ -bonds [15]. As an analogy to this, unpaired centres in the present hafnium and zirconium silicates are also assumed to be terminated by the NO annealing. If this is the case, nitrogen will be observed at the interface. Figure 8 shows depth profiles of the XPS signals due to Hf, Si, O and N atoms obtained for hafnium silicate after the NO postannealing. At the depths from about 60 to 70 nm, the signal due to Si drastically increases, while those due to Hf and O decrease. This region corresponds to the interface between the silicon substrate and the hafnium silicate. Therefore, figure 8 clearly shows that the NO postannealing causes nitridation and effectively diminishes the interface defects.

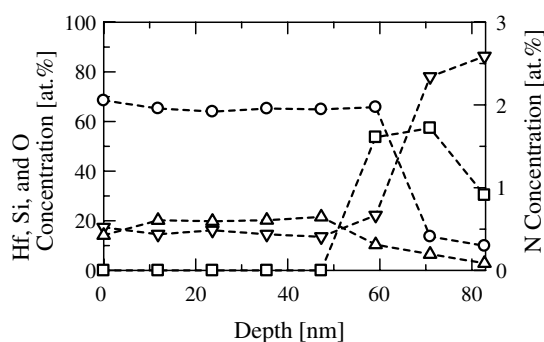


Figure 8. XPS depth profiles of Hf (triangles), Si (inverted triangles), O (circles) and N (squares) atoms obtained for hafnium silicate after the NO postannealing. The broken curves are drawn as a guide for the eyes.

Finally, the possibility of the relevance of any other causes to the decrease in J_{leak} is discussed. It is well known that silicon dioxide is grown at the interface between the high-permittivity dielectric film and the silicon substrate by thermal treatment in O_2 ambient [16]. Furthermore, it has been reported that interfacial oxide layers are also grown in the case of the N_2 annealing [17, 18], probably due to dissolved oxygen and/or reaction with detached oxygen from silicate. The interfacial layer can act as a barrier for carriers, which leads to the decrease in the leakage current. On the other hand, when the film is annealed in NO ambient, NO diffuses into the film and forms strong Si–N bonds at the interface [19–21], which suppresses the formation of interfacial oxide layers [21]. Therefore, the oxide layer thickness grown by the NO annealing must be thinner than that grown by the O_2 or N_2 annealing. This assumption is also supported by the fact that the zirconium silicate deposited in a NO atmosphere has a much thinner interfacial layer than the one deposited in an O_2 atmosphere [16, 22]. Therefore, if the decrease in J_{leak} is due to the growth of the interfacial layer during the postannealing, J_{leak} should be decreased for all the postannealing atmospheres and its reduction ratio should be the smallest in the NO postannealed samples among the three postannealed samples. However, this is not the case in the present result shown in figure 2. Therefore, the decrease in J_{leak} is not due to the growth in the interfacial oxide layer.

To summarize, structural randomness does not affect the electrical properties, while paramagnetic defects such as the P_b centres at the interface act as leakage paths and charge traps. Such defects can be eliminated effectively by nitridation through postannealing in NO ambient.

4. Conclusion

The effects of postannealing on the electrical properties of hafnium and zirconium silicate films deposited on a silicon substrate by PECVD were investigated. For both silicates, the leakage current and the C – V hysteresis width become smaller in the NO and O_2 postannealed samples than in the as-deposited samples, whereas they become larger in the N_2 postannealed samples. In particular, the NO postannealing significantly lowers these values. From FT-IR, ESR and XPS spectroscopy, it has become clear that paramagnetic defects such as the P_b centres at the interface between the film and the substrate are responsible for the leakage current, and that the NO postannealing effectively terminates these defects.

Acknowledgments

This work was partly supported by Grants-in-Aid from the Japan Society for the Promotion of Science (JSPS) for JSPS Fellows (No. 1205733) and for Scientific Research (B) (Nos 12450132 and 16360160). A High-Tech Research Center Grant from the Ministry of Education, Culture, Sports, Science and Technology of Japan is also appreciated.

References

- [1] <http://public.itrs.net>
- [2] Muller D A, Sorsch T, Morrio S, Baunann F H, Lutterodt K E and Timp G 1999 *Nature* **399** 758–61
- [3] Brar B, Wilk G D and Seabaugh A C 1996 *Appl. Phys. Lett.* **69** 2728–30
- [4] Wilk G D, Wallace R M and Anthony J M 2000 *J. Appl. Phys.* **87** 484–92
- [5] Wilk G D and Wallace R M 2000 *Appl. Phys. Lett.* **76** 112–4
- [6] Lee B H, Kang L, Nieh R, Qi W J and Lee J C 2000 *Appl. Phys. Lett.* **76** 1926–8
- [7] Ito T, Kato H, Nango T and Ohki Y 2004 *Japan. J. Appl. Phys.* **43** 8199–202
- [8] Ito T, Kato H and Ohki Y 2006 *J. Appl. Phys.* **99** 094106
- [9] Bhat M, Wristers D J, Han L-K, Yan J, Fulford H J and Kwong D-L 1995 *IEEE Trans. Electron Devices* **42** 907–14
- [10] Ota H, Yasuda N, Yasuda T, Morita Y, Miyata N, Tominaga K, Kadoshima M, Migita S, Nabatame T and Toriumi A 2005 *Japan. J. Appl. Phys.* **44** 1698–703
- [11] Kato H, Seol K S, Fujimaki M, Toyoda T, Ohki Y and Takiyama M 1999 *Japan. J. Appl. Phys.* **38** 6791–6
- [12] Sze S M 1981 *Physics of Semiconductor Devices* (New York: Wiley) p 379
- [13] Devine R A B 1993 *J. Non-Cryst. Solids* **152** 50–8
- [14] Jorgensen C, Svensson C and Ryden K H 1984 *J. Appl. Phys.* **56** 1093–6
- [15] Hegde R I, Tobin P J, Reid K G and Ajuria S A 1995 *Appl. Phys. Lett.* **66** 2882–4
- [16] Ahn H, Chen H-W, Landheer D, Wu X, Chou L J and Chao T-S 2004 *Thin Solid Films* **455/456** 318–22
- [17] Ho M-T, Wang Y, Brewer R T, Wielunski L S and Chabal Y J 2005 *Appl. Phys. Lett.* **87** 133103
- [18] Quevedo-Lopez M A, Chambers J J, Visokay M R, Shanware A and Colombo L 2005 *Appl. Phys. Lett.* **87** 012902
- [19] Lu H C, Gusev E, Yasuda N, Green M, Alers G, Garfunkel E and Gustafsson T 2000 *Appl. Surf. Sci.* **166** 465–8
- [20] Lu H C, Gusev E P, Garfunkel E, Busch B W, Gustafsson T, Sorsch T W and Green M L 2000 *J. Appl. Phys.* **87** 1550–5
- [21] Scheer K C, Rao R A, Muralidhar R, Bagchi S, Conner J, Lozano L, Perez C, Sadd M and White B E Jr 2003 *J. Appl. Phys.* **93** 5637–42
- [22] Chen H-W, Huang T-Y, Landheer D, Wu X, Moisa S, Sproule G I, Kim J K, Lennard W N and Chao T-S 2003 *J. Electrochem. Soc.* **150** C465–71